Published in final edited form as:
J Am Chem Soc. 2008 November 5; 130(44): 14521–14532. doi:10.1021/ja801789t.

Raftlike Mixtures of Sphingomyelin and Cholesterol Investigated by Solid-State ^{2}H NMR Spectroscopy

Tim Bartels[†], **Ravi S. Lankalapalli**[‡], **Robert Bittman**[‡], **Klaus Beyer**[†,§], and **Michael F. Brown**[§,‖,⊥]

Laboratory of Neurodegenerative Disease Research, Ludwig-Maximilian-University, 80336 Munich, Germany, Department of Chemistry and Biochemistry, Queens College of The City University of New York, Flushing, New York 11367, and Department of Biochemistry and Molecular Biophysics, Department of Chemistry, and Department of Physics, University of Arizona, Tucson, Arizona 85721

Abstract

Sphingomyelin is a lipid that is abundant in the nervous systems of mammals, where it is associated with putative microdomains in cellular membranes and undergoes alterations due to aging or neurodegeneration. We investigated the effect of varying the concentration of cholesterol in binary and ternary mixtures with *N*-palmitoylsphingomyelin (PSM) and 1-palmitoyl-2-oleoyl-*sn*-glycero-3-phosphocholine (POPC) using deuterium nuclear magnetic resonance (^{2}H NMR) spectroscopy in both macroscopically aligned and unoriented multilamellar dispersions. In our experiments, we used PSM and POPC perdeuterated on the *N*-acyl and *sn*-1 acyl chains, respectively. By measuring solid-state ^{2}H NMR spectra of the two lipids separately in mixtures with the same compositions as a function of cholesterol mole fraction and temperature, we obtained clear evidence for the coexistence of two liquid-crystalline domains in distinct regions of the phase diagram. According to our analysis of the first moments M_1 and the observed ^{2}H NMR spectra, one of the domains appears to be a liquid-ordered phase. We applied a mean-torque potential model as an additional tool to calculate the average hydrocarbon thickness, the area per lipid, and structural parameters such as chain extension and thermal expansion coefficient in order to further define the two coexisting phases. Our data imply that phase separation takes place in raftlike ternary PSM/POPC/cholesterol mixtures over a broad temperature range but vanishes at cholesterol concentrations equal to or greater than a mole fraction of 0.33. Cholesterol interacts preferentially with sphingomyelin only at smaller mole fractions, above which a homogeneous liquid-ordered phase is present. The reasons for these phase separation phenomena seem to be differences in the effects of cholesterol on the configurational order of the palmitoyl chains in PSM-d_{31} and POPC-d_{31} and a difference in the affinity of cholesterol for sphingomyelin observed at low temperatures. Hydrophobic matching explains the occurrence of raftlike domains in cellular membranes at intermediate cholesterol concentrations but not saturating amounts of cholesterol.

E-mail: mfbrown@u.arizona.edu.
[†]Ludwig-Maximilian-University.
[‡]Queens College of The City University of New York.
[§]Department of Biochemistry and Molecular Biophysics, University of Arizona.
[‖]Department Chemistry, University of Arizona.
[⊥]Department of Physics, University of Arizona.

Supporting Information **Available:** Complete lists of the spectral assignments as well as the structural parameters obtained using the first-order mean-torque model. This material is available free of charge via the Internet at http://pubs.acs.org.

Introduction

The concept that biomembranes are two-dimensional fluids with randomly distributed proteins has been challenged by the proposal that cellular membranes may contain areas of lateral segregation known as lipid rafts.[1] The presence of these domains is typically associated with cellular functions such as vesicle fusion, signal transduction, lipid trafficking, transcytosis, protein sorting, and virus budding.[2] Hence, they constitute an important target for research in pharmaceutical and physical chemistry as well as in cellular biology. As currently understood, rafts are mostly depleted of unsaturated phospholipids and enriched in sphingolipids, cholesterol, and certain lipid-anchored proteins.[3] Sphingomyelin is abundant in the nervous systems of mammals and undergoes compositional changes due to aging or neurodegeneration. The observation that depletion of cholesterol from biological membranes induces major changes in the distribution and function of raft-associated proteins[4] indicates that cholesterol is an essential component of raft domains. However, a thorough investigation of the physical basis for these observations is complicated by the intricate lipid compositions of most biological membranes. It is therefore desirable to further illuminate the physical properties of lipids in simple raftlike model systems.

Raftlike domains are believed to occur in lipid systems with coexisting liquid-disordered (l_d) and liquid-ordered (l_o) phases.[5,6] The l_o phase is characterized by a high rate of transverse diffusion and positional disorder, as found in the l_d phase, together with relatively ordered acyl chains, as occurs in the solid-ordered (s_o) phase.[5,7] The l_d phase in these systems typically contains highly unsaturated lipids with a low phase-transition temperature, whereas the l_o phase predominately consists of a saturated or sphingolipid component with a high phase-transition temperature and cholesterol. Analyzing the thermodynamics and structural properties of such lipid mixtures remains a challenging task.[8] Experiments using fluorescence techniques have led to substantial progress in understanding the phase behavior and boundaries in ternary mixtures by their ability to establish binary and ternary phase diagrams for several lipid systems of current interest.[9] Yet these phase diagrams are often quite fragmentary at physiologically relevant temperatures and in some cases can lead to questionable conclusions because of the need to incorporate a fluorescent probe. This last disadvantage has recently attracted significant attention, as changes in phase behavior have been discovered upon addition of even trace amounts of a fluorescent probe.[10]

Solid-state ^{2}H NMR spectroscopy, on the other hand, is a versatile technique that lends itself to a noninvasive investigation of the order and mobility of acyl chains and polar headgroups in lipid bilayers.[11,12] The residual quadrupolar couplings (RQCs) of chain deuterons located within the lipid bilayer can be evaluated in terms of segmental order parameters and order parameter distributions, which may also yield knowledge about partitioning of the lipids into different bilayer domains. Further interpretation using structural models can provide information on the mean interfacial area of a lipid or the average length of the acyl chain projection, which is directly related to the membrane thickness.[12,13] Combining these measurements with the overall ordering of the acyl chains, which is directly accessible by solid-state ^{2}H NMR experiments, enables one to acquire information about the phase behavior of lipids in the mixtures. Nonetheless, a limitation of this technique is the availability of selectively deuterated lipid samples. Deuteration of sphingomyelin is of particular interest because of the abundance of this lipid in the nervous systems of mammals, where it becomes increasingly enriched as a result of progression in age,[14] but it poses a synthetic challenge. The normal semisynthetic pathway, namely, removal of the amide-linked fatty acyl chain followed by reacylation with a deuterated derivative, is hampered by partial epimerization at the C3 carbon of the sphingosine backbone. Despite these difficulties, a chemical synthesis of optically pure and selectively ^{2}H-labeled sphingomyelin is needed for an investigation of the putative role of sphingomyelin in the formation of rafts.

In our studies, we used binary mixtures of cholesterol with 1-palmitoyl-2-oleoyl-*sn*-glycero-3-phosphocholine (POPC) or *N*-palmitoylsphingomyelin (PSM), in which the palmitoyl chain of POPC or PSM was perdeuterated, to study the different effects of cholesterol on the saturated chains of the lipid. Additionally, we investigated ternary mixtures containing both lipids and varying cholesterol content at several temperatures in order to obtain structural information on the lipids for representative sections of the phase prism of the ternary mixture. We observed each ^{2}H-labeled lipid component separately, and using a structural model, we were able to distinguish the order parameter profile for each component in its respective phase. For certain ranges of temperature and cholesterol content, lateral phase separation due to the preferential interaction of cholesterol with sphingomyelin was demonstrated. However, our data suggest that little or no phase separation is detectable at cholesterol mole fractions (X_C) greater than 0.33, indicating that PSM is in a homogeneous phase with POPC and cholesterol. These concentrations are lower than those implied by published phase diagrams[9,15] and have important implications for lateral organization and raft formation in biological membranes in vivo.

Methods

Chemicals

Synthetic POPC, egg yolk sphingomyelin (EYSM), cholesterol, and 1-perdeuteriopalmitoyl-2-oleoyl-*sn*-glycero-3-phosphocholine (POPC-d_{31}) were purchased from Avanti Polar Lipids (Alabaster, AL). Perdeuterated palmitic acid (palmitic acid-d_{31}) and deuterium oxide were obtained from Cambridge Isotopes (Promochem GmbH, Wesel, Germany). Labeled *N*-perdeuteriopalmitoylsphingomyelin (PSM-d_{31}) was synthesized by N-acylation of D-*erythro*-sphingosylphosphocholine as described previously.[16] Briefly, the *p*-nitrophenyl ester of palmitic acid-d_{31} and anhydrous potassium carbonate were added to lysosphingomyelin (prepared from EYSM as previously described[17]) in a mixture of anhydrous dimethylformamide and dichloromethane under nitrogen, and the mixture was stirred at ambient temperature for 1 day. The products were purified by silica gel column chromatography (eluting with 65:35:5 chloroform/methanol/water), and the suspended silica gel was removed by filtration. Purity was checked by thin-layer chromatography and liquid chromatography/mass spectrometry.

Lipid Sample Preparation

Oriented lipid multibilayers were prepared and macroscopically aligned as described elsewhere.[18,19] Briefly, 30 mg of the lipid or lipid mixture containing at least 12 mg of deuterated material was dissolved in 2.5 mL of *tert*-butyl alcohol. The solution was spread onto 50 ultrathin glass plates (8.3 × 18.3 × 0.08 mm; Marienfeld Laboratory Glassware, Lauda-Königshofen, Germany) and dried for 20 min under a stream of warm air and then at room temperature for at least 18 h in vacuo (20−30 Pa). The glass plates were stacked on top of each other with gentle pressure and inserted, along with a pair of glass cylinder segments, into an open glass tube (inner diameter 9.8 mm). Two small paper strips were soaked in ^2H_2O and carefully dried in order to exchange labile hydrogen for deuterium. The strips were attached to the short sides of the glass stacks, and a few microliters of ^2H_2O or a 10:90 (v/v) ^2H_2O/H_2O mixture was applied to the paper surface. The tube was rapidly sealed with two appropriately machined Teflon plugs having silicon O-rings. The membranes were annealed for 8 h at 46 °C. The annealing process and the final hydration level were monitored by observation of the water signal at the offset frequency of the ^{2}H NMR spectrum.[19]

For unoriented samples, the lyophilized (from *tert*-butyl alcohol) lipid mixture containing at least 20 mg of perdeuterated material was weighed in a glass tube, and 50 wt % of ^{2}H-depleted water was added. On one side of the tube, a constriction was drawn by heating the glass with

an oxygen burner under Ar. Immediately thereafter, the top of the constriction was melted and thereby sealed under vacuum. While the glass was heated, the sample was held at 77 K in a bath of liquid nitrogen. The tube was centrifuged at 5000*g* with inversion of the sample several times above the phase-transition temperature in order to ensure complete hydration. After equilibration for at least 4 h, both sides of the tube were opened with a glass cutter, and the sample was transferred to a tubular polycarbonate jacket with a diameter of 5 mm by applying gentle pressure to the nonconstricted end. The jacket was sealed with appropriately machined Teflon plugs. Because of the use of ^{2}H-depleted water and the consequent absence of the water signal, the annealing was monitored by the overall shape of the spectra above the phase-transition temperature.

Solid-State Deuterium NMR Spectroscopy

All of the ^{2}H NMR spectra were acquired with a Varian VXR-400 spectrometer operating at 9.4 T (^{2}H frequency 61.4 MHz). Spectra of macroscopically aligned samples were obtained using a 10 mm flat-wire solenoid. A locally constructed goniometer was used for accurate alignment in the magnetic field at $\theta = 0°$, where θ denotes the angle between the normal to the bilayer stack and the field direction.[19] In some cases, it was more practical to acquire spectra of powder-type samples using a 5 mm flat-wire solenoid, which were de-Paked using rapid deconvolution by weighted fast Fourier transformation[20] to yield results for the $\theta = 0°$ orientation. The quadrupolar echo sequence[21] was applied for signal excitation, using composite pulses with a 90° pulse width of 10 μs for the 10 mm coil and 3 μs for the 5 mm coil. The pulse spacing was 20 μs, and the recycle delays were chosen to avoid saturation. To increase the signal-to-noise ratio, the unoriented spectra were symmetrized by processing only the data points recorded from the real channel. When samples of several compositions were measured with both experimental setups, the results were in good agreement, giving almost identical quadrupolar splittings and ^{2}H NMR spectra. Order parameters for individual carbon positions in the *N*-palmitoyl chain of PSM-d_{31} or the *sn*-1 chain of POPC-d_{31} were obtained from the resolved quadrupolar splittings $\Delta\nu_Q^{(i)}$ according to eq 1:

$$|\Delta\nu_Q^{(i)}| = \frac{3}{2}\chi_Q |P_2(\cos\theta)\| S_{CD}^{(i)}| \quad (1)$$

where χ_Q denotes the quadrupolar coupling constant (167 kHz for a C–^{2}H bond), $P_2(\cos\theta)$ is the second Legendre polynomial, and $S_{CD}^{(i)}$ is the order parameter for the *i*th C-^{2}H bond in the hydrocarbon chain. The quadrupolar splittings of the C2 methylene groups were omitted because of their inequivalence; the almost parallel alignment to the membrane surface of the *pro-R* deuteron and the ~34° angle of the *pro-S* deuteron in the case of 1,2-dipalmitoyl-*sn*-glycero-3-phosphocholine (DPPC) does not allow a comparison with the other methylene segments. Peak assignments were generally made by assuming that the order parameters decrease in going from C3 to the methyl end and that the area under each peak is proportional to the number of deuterons. A more precise assignment of the ^{2}H NMR spectra of pure PSM-d_{31} and PSM-d_{31}/POPC was possible on the basis of previously published results.[16,17]

For the oriented samples, the number of water molecules per lipid headgroup (n_w) was obtained by calculating the integral ratio of the respective ^{2}H signals from ^2H_2O and the labeled lipids. The hydration level was adjusted to obtain full hydration[23] of the respective bilayers ($25 \leq n_w \leq 35$). The angle θ between the normal to the glass plates and the magnetic field was varied until the quadrupolar splittings $\Delta\nu_Q^{(i)}$ reached a maximum, indicating that $\theta = 0°$ (eq 1). In the case of the unoriented samples, the addition of 50 wt % of water assured complete hydration

for the duration of the experiments. For the unoriented samples, the first and second moments M_n (n = 1, 2) were calculated according to eq 2:

$$M_n = \frac{\int_0^\infty \omega^n f(\omega) \quad d\omega}{\int_0^\infty f(\omega) \quad d\omega} \tag{2}$$

where $f(\omega)$ denotes the spectral intensity distribution and $\omega = 0$ corresponds to the Larmor frequency ω_0.

Calculation of Structural Parameters via Application of the First-Order Mean-Torque Model

If it is assumed that the hydrocarbon chains have an average shape of a prism (cylinder or cuboid), the distance traveled between carbons $i + 1$ and $i - 1$ projected on the bilayer normal can be expressed as

$$D_i = \frac{2V_{CH_2}}{A_i} \tag{3}$$

where A_i is the cross-sectional area per segment and V_{CH_2} is the volume of a single methylene group, which can be approximated using the expression $V_{CH_2}(T) \approx V^0_{CH_2} + \alpha_{CH_2}(T - 273.15 \quad \text{K})$,[13] in which the empirical parameters $V^0_{CH_2}$ and α_{CH_2} have the values 26.5 Å^3 and 0.0325 Å^3/K, respectively. The distance D_i, which is twice the travel of one methylene group, can be expressed in terms of the theoretical maximum projection of the vector connecting the two neighboring carbon atoms of the segment i onto the bilayer normal (D_M = 2.54 Å) and the angle β_i between the vector and the bilayer normal: $D_i = D_M \cos \beta_i$. The average travel of the carbon segment is therefore given by eq 4:

$$\langle D_i \rangle = D_M \langle \cos \quad \beta_i \rangle \tag{4}$$

This result enables the average projected chain length $\langle L^*_C \rangle$, which gives the average distance between the second carbon and the terminal methyl group, to be calculated by summing up the projections for each carbon segment:

$$\langle L^*_C \rangle = \sum_{i=3,5\ldots}^{n_C - 1} \langle D_i \rangle \tag{5}$$

where n_C designates the number of carbons per chain. We can also determine the full chain length projection $\langle L_C \rangle$ by estimating $\langle D_2 \rangle$ by $\langle D_3 \rangle$ and adding the extra term $\langle D_{n_C - 1} \rangle$ to approximate the contribution from the n_C = 16 terminal methyl end:

$$\langle L_C \rangle = \frac{1}{2} \sum_{i=2}^{n_C - 1} \langle D_i \rangle + \langle D_{n_C - 1} \rangle \tag{6}$$

It should be stressed that the hydrophobic thickness and the chain length are not necessarily the same because of the existence of a distribution of acyl chain lengths and interdigitation between opposing bilayers. Although it is possible to determine the average projected chain

length by summing up the projection contributions for each carbon segment, the hydrocarbon thickness D_C can be calculated by using just the values obtained for the plateau-region carbon segments, which gives results in good agreement with available X-ray data.[13]

With the assumption that the average shape of the hydrocarbon chain constitutes a geometrical prism, the volumetric thickness D_C is then related to $\langle A \rangle$ by the expression

$$D_C = \frac{2V_C}{\langle A \rangle} \tag{7}$$

where V_C is the total volume of a single chain. It is well established that the volume of a methyl group is twice the methylene volume,[24] i.e., $V_{CH_3} \approx 2V_{CH_2}$. Moreover, for the top part of the chain (nearest the aqueous interface), eq 3 can be rewritten as:

$$\langle A \rangle = \frac{2V_{CH_2}}{D_M} \left\langle \frac{1}{\cos \beta} \right\rangle \tag{8}$$

In the above formula, $\langle A \rangle$ represents the mean area per chain at the aqueous interface and β corresponds to those segments in the plateau region of the order profile where $S_{CD} \approx$ constant (index i is suppressed). Hence, using eqs 7 and 8, we express D_C as

$$D_C = \frac{1}{2} n_C D_M \left\langle \frac{1}{\cos \beta} \right\rangle^{-1} \tag{9}$$

For calculation of the average interfacial area $\langle A \rangle$ and the hydrocarbon thickness D_C, the value of the so-called area factor $q = \langle 1/\cos \beta \rangle$ is needed; it can be approximated by[13]

$$q \approx 3 - 3\langle \cos \beta \rangle + \langle \cos^2 \beta \rangle \tag{10}$$

For individual segments (index i), obtaining the value of $\langle \cos^2 \beta_i \rangle$ from the RQCs is straightforward using eq 11:

$$\langle \cos^2 \beta_i \rangle = \frac{1 - 4S_{CD}^{(i)}}{3} \tag{11}$$

Solid-state ^{2}H NMR experiments enable the order parameter $|S_{CD}|$ for the plateau region to be obtained directly from observables using eq 1.

However, in the liquid-crystalline state, acquiring the value of $\langle \cos \beta_i \rangle$ is more complicated because $\langle \cos^2 \beta_i \rangle^{1/2} \neq \langle \cos^2 \beta_i \rangle$, which manifests the variance of the length and area distributions.[25] In effect, one needs to know the first and second moments of the orientational distribution function $f(\beta)$. For statistical treatment of the possible orientational angles β, the mean-torque model assumes that the orientational order of the acyl chain segments relative to the local director frame can be described by a mean-field orientational potential, denoted by $U(\beta)$, which in a first-order approximation is given by $U(\beta) \approx U_1 \cos \beta$. The form of the distribution function of β is given by the Boltzmann factor, yielding

$$f(\beta) = \frac{1}{Z}\exp\left(-\frac{U(\beta)}{k_B T}\right) \tag{12}$$

in which the partition function is

$$Z = \int_0^{\pi} \exp\left(-\frac{U(\beta)}{k_B T}\right) \sin \beta \, d\beta \tag{13}$$

If a first-order mean-torque potential is assumed, the following coupled equations, obtained from integration of eqs 12 and 13 by cos β, can be solved numerically:

$$\langle \cos \beta \rangle = \coth\left(-\frac{U_1}{k_B T}\right) + \frac{k_B T}{U_1} \tag{14}$$

$$\langle \cos^2 \beta \rangle = 1 + 2\left(-\frac{k_B T}{U_1}\right)^2 + \frac{2k_B T}{U_1} \coth\left(-\frac{U_1}{k_B T}\right) \tag{15}$$

An analytical solution for $\langle \cos \beta \rangle$ can then be obtained using the approximation $\coth(-U_1/k_B T) \approx 1$, which for individual segments gives the relation

$$\langle \cos \beta_i \rangle = \frac{1}{2}\left(1 + \sqrt{\frac{-8S_{CD}^{(i)} - 1}{3}}\right) \tag{16}$$

It should be noted that in the limit of an all-trans chain with axial symmetry, $\langle \cos^2 \beta_i \rangle = \langle \cos \beta_i \rangle = 1$, giving $q = 1$. Hence, according to eqs 8 and 9, the limiting area is $2V_{CH_2}/D_M$ and the limiting volumetric thickness is $n_C D_M/2$, suggesting that the model can also be applied to the gel state at temperatures where rotational diffusion of the lipids occurs. Although the above formula is applicable only for order parameters $S_{CD}^{(i)} \leq -1/8$, this is sufficient for most plateau values in ^{2}H NMR of lipid membranes. For the calculation of $\langle \cos \beta_i \rangle$ in cases of smaller order parameters, eqs 14 and 15 are applied. Use of the mean-torque model is justified mainly for large $|S_{CD}|$ values, but nonetheless, calculating the chain length of highly mobile methylene groups with small absolute magnitudes of the order parameter can be a valuable tool, especially for comparing data for the same acyl chains at different temperatures and in different mixtures. For a mixture, the area factor q is the weighted sum and the calculated values of D_C and $\langle A \rangle$ are then number-weighted averages over the components, according to the theory of moments. Lastly, from the values of D_C and $\langle A \rangle$, the isobaric thermal expansion coefficients parallel ($\alpha_\parallel$) and perpendicular ($\alpha_\perp$) to the membrane normal can be calculated using eqs 17 and 18, respectively:

$$\alpha_\parallel = \frac{1}{D_C}\left(\frac{\partial D_C}{\partial T}\right)_p \tag{17}$$

$$\alpha_{\perp}=\frac{1}{\langle A\rangle}\left(\frac{\partial\langle A\rangle}{\partial T}\right)_{P} \quad (18)$$

Results

Deuterium NMR Spectroscopy of Binary Lipid Mixtures Containing Cholesterol

Phosphatidylcholines and sphingomyelins from cell and organelle membranes are characterized by distinct physical and spectroscopic properties, regardless of their common choline headgroup. Figure 1a,b compares ^{2}H NMR spectra of PSM-d_{31} and POPC-d_{31} with decreasing temperature. PSM-d_{31} shows a sharp liquid-crystalline-to-gel phase transition in the narrow temperature range 36−38 °C (indicative of high sample purity), with a remarkably large maximum RQC of 72.3 kHz (for θ = 0° in eq 1) in the l_d state at 40 °C (Figure 1a). The deviation from the published phase-transition temperature of PSM (T_m = 41.5 °C) is a consequence of the perdeuteration of the acyl chain, which is known to decrease the chain-melting temperatures.[26] In contrast, a spectrum indicating liquid-crystalline POPC-d_{31} is obtained over the whole temperature range of the measurement, with the largest RQC being 54.8 kHz (θ = 0°) at 15 °C, in good agreement with previous results[27] (Figure 1b). The gel phase of PSM-d_{31} is distinguished by a broad doublet with a maximum splitting of 117.0 kHz (for θ = 0°) at 15 °C. This is consistent with axial rotation of the lipids at temperatures moderately below that of the phase transition, with little or no biaxiality.

In an equimolar mixture of sphingomyelin and POPC, the phase transition commences at 25 °C and is not complete at 15 °C. The transition can be directly seen in the mixture containing PSM-d_{31} by the emergence of additional gel-phase signals with a quadrupolar splitting of 105.8 kHz at θ = 0° (Figure 1c). The spectrum of PSM-d_{31} in the liquid-crystalline state is still superimposed on the gel-state spectrum, indicating that both phases coexist at 15 °C. The observation of distinct ^{2}H NMR spectral components implies that the lateral phase segregation entails a domain size large enough for diffusional exchange of the deuterated lipids between the domains to be slow on the ^{2}H NMR time scale. In contrast, there is only one component in the ^{2}H NMR spectra of POPC-d_{31} in the same binary mixture (Figure 1d), suggesting that this phospholipid rapidly exchanges between ordered and disordered domains. It may be seen that the POPC-d_{31} spectrum broadens significantly at 25 °C, i.e., close to the phase transition identified in Figure 1c. One should also note that because of the limited availability of chemically defined PSM, use of EYSM/POPC-d_{31} mixtures could yield slightly different phase behavior compared to PSM-d_{31}/POPC mixtures. However, the fraction of PSM in EYSM is sufficiently large (84%), and the major changes in PSM-d_{31}/POPC membranes are reflected in EYSM/POPC-d_{31} mixtures at the same temperatures (see below), implying that substitution of EYSM for PSM has only a small influence.

For an assessment of the effect of cholesterol on the palmitoyl chains of PSM and POPC in ternary mixtures, we first studied the cholesterol–lipid interaction for each lipid component separately. Therefore, solid-state ^{2}H NMR spectra were obtained for PSM-d_{31} or POPC-d_{31} bilayers containing various cholesterol concentrations over a range of temperatures. The spectra of PSM-d_{31}/cholesterol mixtures (Figure 2) differ substantially from those of PSM-d_{31} alone. At the lowest cholesterol mole fraction, X_C = 0.15, the quadrupolar splitting corresponding to the outer edges of the spectrum increases by 15 kHz at 55 °C, which can be attributed to the well-known ordering effect of the rigid cholesterol ring structure.[28-30] This is accompanied by signal broadening, which to some extent may be the result of rapid exchange of the lipids between ordered and liquid-disordered domains. Inhomogeneous line broadening, due, for example, to a more pronounced mosaic spread in the macroscopically oriented samples,

must be also considered. The entire phase transition is substantially broadened in this case, i.e., the onset can be detected at 42 °C, and completion has not been reached at 20 °C (Figure 2a). When the cholesterol content is increased to $X_C = 0.2$, the transition from the l_d to the s_o phase seems to vanish completely. The significant line broadening and the increased splittings suggest the coexistence of an l_d phase and a new l_o phase instead of the s_o phase, with the l_d phase prevailing. The spectra at 38 °C shown in Figure 2b display a shift of the phase equilibrium from the l_d phase toward the l_o phase, which becomes the main phase below 35 °C. This trend is continued at a mole fraction of $X_C = 0.25$ (Figure 2c), with the phase transition being less notable and already begun at 45 °C.

Finally, at $X_C = 0.33$, the main phase transition is no longer detectable, and the ^{2}H NMR spectrum at 55 °C reflects a homogeneous l_o state (Figure 2d). Thus, at $X_C = 0.33$, the amount of cholesterol seems to be sufficient to completely eliminate the l_d phase in a binary mixture with sphingomyelin. In addition, at 40 °C the largest splitting shifts from 65.7 kHz for PSM-d_{31} alone to 104.8 kHz ($\theta = 0°$), corresponding to an order parameter of $S_{CD} = 0.42$, which is indicative of an l_o state. The large quadrupolar splitting is close to the calculated maximum splitting of 127.5 kHz expected for complete parallel alignment of the acyl chains with respect to the magnetic field when in the trans state and rotating about the bilayer normal.

A comparison with the ^{2}H NMR spectrum of an analogous POPC-d_{31}/cholesterol mixture ($X_C = 0.33$) reveals further differences (Figure 3). The splittings at lower temperatures reflect similar chain ordering for the POPC-d_{31} and PSM-d_{31} bilayers. In the former system, however, the splittings decrease much faster with temperature, reaching 66.5 kHz at 60 °C, which is more akin to a mixture of l_d and l_o phases rather than to a pure l_o state. However, compared to those for PSM-d_{31}, the signals in the POPC-d_{31} spectra are much better resolved in both the oriented and powder-type samples, most probably as a consequence of the fluidizing effect of the adjacent oleoyl chain on the palmitoyl chain. We thus conclude that cholesterol at concentrations below a mole fraction of $X_C = 0.33$ has less influence on the ordering of the palmitoyl chain of POPC than on ordering of the sphingomyelin *N*-palmitoyl chain. A more detailed study of the POPC-d_{31}/cholesterol system using ^{2}H NMR techniques has recently been published elsewhere.[31,32]

Order Parameter Profiles of Binary Lipid – Cholesterol Mixtures

Order parameter profiles derived from the quadrupolar splittings for PSM-d_{31} and POPC-d_{31} and for binary mixtures of these lipids with cholesterol are shown in Figure 4. A general feature of the profiles is the decrease of the order parameters with increasing distance from the lipid–water interface. However, the profiles clearly reveal distinct differences between the lipids. For example, for POPC-d_{31} alone at 45 and 60 °C (Figure 4d), the almost identical splittings of the interfacial chain segments give rise to an order parameter plateau, whereas the same chain positions for PSM-d_{31} (Figure 4a) are characterized by slightly decreasing order parameters.

The distinction between the sphingo- and glycerophospholipids becomes even more conspicuous in the presence of cholesterol. For PSM-d_{31}, the profile changes drastically in the presence of 20 mol % of cholesterol. At 45 and 60 °C, a broad unresolved doublet now appears, i.e., there is a plateau region comprising ~10 methylene segments. The quadrupolar splittings from the interfacial segments increase at temperatures <40 °C, yielding an order parameter close to the value of −0.5 that would be expected for hydrocarbon chains in an all-trans state. At 33 mol % of cholesterol, the high-temperature order parameters for all of the PSM-d_{31} segments increase significantly, and the ordering profiles are much less temperature-sensitive. In sharp contrast, there is no sudden increase in order parameter with decreasing temperature for POPC-d_{31} at a cholesterol concentration of 20 mol %. Moreover, the temperature dependence of the profiles is stronger with increasing cholesterol content. At 33 mol %

cholesterol, the plateau order parameter values vary from 0.42 to 0.26 on going from 20 to 60 °C, which may be contrasted to the variation from 0.46 to 0.37 observed for PSM-d_{31}. The numerical RQCs for the $\theta = 0°$ orientation and their assignments to the respective carbon segments are provided in the Supporting Information.

Deuterium NMR Spectroscopy of Ternary Mixtures and Moment Analysis

A simple model for elucidating the physical properties of lateral inhomogeneities in biological membranes, often called lipid rafts, is a ternary mixture comprising sphingomyelin, POPC, and cholesterol. Figure 5 compares the ^{2}H NMR spectra acquired for ternary mixtures of PSM, POPC, and cholesterol at a series of different temperatures. The addition of cholesterol at a mole fraction of $X_C = 0.2$ has a major impact on the spectra of PSM-d_{31} in ternary mixtures with POPC (1:1), as shown in Figure 5a. The plateau splitting at higher temperatures (71.3 kHz at 60 °C for $\theta = 0°$) falls between the RQC values obtained for binary mixtures of PSM-d_{31} and POPC (56.6 kHz at 55 °C for $\theta = 0°$; not shown) and those for PSM-d_{31}/cholesterol with $X_C = 0.33$ in the l_o phase (91 kHz for $\theta = 0°$ at 60 °C; not shown). At 35 °C, an extensive line broadening becomes noticeable and persists to 15 °C (Figure 5a). In contrast, the POPC-free binary mixture of PSM-d_{31} and cholesterol with $X_C = 0.20$ (Figure 2b) shows the same phase transition, but with only a small range of phase coexistence near 40 °C that merges near 35 °C to give an l_o phase at lower temperatures. This difference in phase behavior indicates that the addition of POPC seems to destabilize the formation of an l_o phase, therefore delaying and prolonging the l_d-to-l_o phase transition.

Interestingly, in Figure 5a, the methyl group signal consists of doublet splittings (17.7 and 11.0 kHz for $\theta = 0°$, respectively), which are attributed to the coexistence of two laterally separated phases with different lipid compositions.[32] When the system is cooled from 60 °C, the doublets appear at ~38 °C. This subset of splittings indicates that the phase domains are large enough to yield discrete spectral components on the ^{2}H NMR time scale. According to the integral ratio of the methyl peaks (Figure 5a), the main fraction of PSM-d_{31} is in the l_o phase with a quadrupolar splitting of 17.7 kHz, while the smaller fraction pertains to an l_d phase characterized by a splitting of 11.0 kHz. A comparison of the ternary PSM-d_{31} spectra with those obtained with POPC-d_{31} (shown in Figure 5b) displays similarities and differences in the methyl group splittings. As lower temperatures are reached, the appearance of a second phase with domains large enough to generate a separately observable spectrum on the ^{2}H NMR time scale becomes evident for the mixture containing 1:1 POPC-d_{31}/EYSM with $X_C = 0.2$. At 30 °C, the second phase becomes noticeable by a sudden broadening of the methylene peaks. At 25 °C, a second set of plateau peaks appears, with a splitting of ~96 kHz for $\theta = 0°$, indicating a partitioning of POPC into the l_o phase formed by PSM and cholesterol. A closer look at the inset in Figure 5b again shows doublet splittings for the methyl group signal, which arise from the main peak (8.8 kHz) and lead to a well-resolved second peak (11.5 kHz), indicating a spectral component due to the segregated POPC fraction in the l_o phase. The integral ratio of the two peaks, which changes in the temperature range 25−15 °C in favor of the outer methyl peak, further substantiates this point. Interestingly, the integral ratio is reversed in comparison with the methyl group splitting seen for 1:1 PSM-d_{31}/POPC with $X_C = 0.2$ (Figure 5a). For 1:1 POPC-d_{31}/EYSM with $X_C = 0.2$ (Figure 5b), the main fraction of POPC-d_{31} is in the l_d phase, as the outer peak at 8.8 kHz is larger, and the smaller part of the lipid fraction partitions into an l_o phase with PSM-d_{31}, as indicated by the smaller peak at 11.5 kHz. When the cholesterol content is increased to $X_C = 0.33$ (Figure 5c) the ^{2}H NMR spectra of PSM-d_{31} in a ternary mixture with POPC and cholesterol become simpler, with splittings similar to the binary mixtures of PSM-d_{31} with $X_C = 0.33$. The splittings correspond to an l_o phase over almost the whole temperature range studied. Nonetheless, the broadening of the peaks at 60 °C again may indicate the emergence of a second liquid-crystalline phase at higher temperatures. Additionally, the overall decrease in the splittings of the plateau peaks for the ternary 1:1 PSM-

d_{31}/POPC mixture with $X_C = 0.33$ (95.2 kHz for $\theta = 0°$ at 40 °C; Figure 5c) compared with those for the binary mixture of PSM-d_{31} with $X_C = 0.33$ (104.8 kHz at 40 °C; not shown) imply that significant amounts of POPC are incorporated in the l_o phase. This leads to smaller quadrupolar splittings for PSM-d_{31} and hence to diminished average order in the ^{2}H-labeled palmitoyl chain.

Next, the complementary experiment employed POPC-d_{31} instead of PSM-d_{31} in the same ternary system ($X_C = 0.33$), as shown in Figure 5d. This lipid also exhibits uniform ^{2}H NMR spectra with large methyl group splittings (89.9 kHz for $\theta = 0°$ at 40 °C for the plateau peak), which are even greater than those in binary mixtures with cholesterol alone (85.0 kHz at 40 °C; not shown). The presence of sphingomyelin seems to have an additional ordering effect on the palmitoyl chain in POPC, which leads to increased quadrupolar splittings in a ternary PSM/POPC-d_{31}/cholesterol mixture in comparison with a binary POPC-d_{31}/cholesterol mixture at the same total cholesterol molar ratio ($X_C = 0.33$). This observation is in line with almost ideal mixing of POPC and sphingomyelin in these mixtures. Another noticeable feature is the remarkably high resolution of individual resonances with lower quadrupolar splittings for the nonplateau methylene groups (C11 to C15) in the palmitoyl chain of POPC-d_{31} in comparison with PSM-d_{31}. This is a general feature of the POPC spectra, as already shown in the binary mixtures with POPC-d_{31} and cholesterol alone. The unsaturated *sn*-2 chain of POPC obviously has a disordering effect on the later methylene groups in the acyl chain, probably due to the double bond in the oleoyl chain. Values of the quadrupolar splittings for the $\theta = 0°$ orientation and their segmental assignment are provided in the Supporting Information.

The first spectral moments M of the ^{2}H NMR spectra (eq 2) are shown in Figure 6 and reflect the average orientational order in the bilayer membrane as a function of temperature. The plots of M_1 versus temperature again show the clear difference between POPC-d_{31} and PSM-d_{31} with $X_C = 0.2$, as seen in Figure 6a. Obviously, PSM is situated in an environment of higher segmental order on average, while the palmitoyl chain of POPC is highly mobile. This underscores the coexistence of the two phases, one formed by an l_d mixture of POPC and cholesterol with a very low PSM content and the other consisting of l_o domains that are rich in PSM and cholesterol and almost depleted of POPC. At a cholesterol concentration of $X_C = 0.33$ (Figure 6b), the differences between the two first spectral moments vanish almost completely, giving values characteristic of an l_o phase for both lipids. There is a divergence of the moments only at higher temperatures, most likely because POPC begins to form an l_d phase earlier than PSM. This strongly argues for ideal mixing of the lipids at temperatures below 50 °C with cholesterol mole fractions of $X_C = 0.33$.

Discussion

Dynamical Structure and Chain Packing of Lipid-Raft Components

Analysis of the ^{2}H NMR data by means of the first-order mean-torque model[13] is very useful for gaining an understanding of the forces affecting membrane lipid bilayers. This approach can be used to determine the average projected length onto the bilayer normal for each segment of the acyl chain, thereby allowing calculation of the average carbon position relative to an arbitrary reference point (here, the terminal methyl group). Accordingly, we reindex the carbon atoms i using the alternate index $i' = n_C - i + s$, where s is an arbitrary shift value. For $s = 2$, the indexing is reversed, giving $i' = 2$ for the terminal methyl group and $i' = 16$ for the C2 carbon. This is more convenient for direct comparison of the headgroup region. The chain-extension profiles obtained in such a manner facilitate the analysis of the different bilayer structures. Applying this approach to binary mixtures of PSM-d_{31} or POPC-d_{31} with cholesterol allows a comparison of the specific ordering effects of cholesterol on these lipids, thus revealing the factors leading to lipid mixing or phase separation.

In Figure 7 we compare the effects of cholesterol on the cumulative projected chain length at the level of single-carbon segments of the PSM-d_{31} palmitoyl chain. At lower temperatures (20 and 30 °C), the l_o phase is assumed for a sphingomyelin membrane with $X_C = 0.33$, whereas the gel phase is adopted for pure PSM-d_{31}. In both cases, however, the chain-extension profiles exhibit nearly identical characteristics with regard to the segmental projections onto the bilayer normal (Figure 7a,b). Although the narrow line shape of the ^{2}H NMR spectra of PSM-d_{31} with $X_C = 0.33$ (Figure 2d) clearly indicates the existence of a homogeneous l_o phase over the whole temperature range, the chain extensions shown in Figure 7a,b are almost the same as in the s_o gel phase, which is identified by the line shape of the ^{2}H NMR spectra for pure PSM-d_{31} at 15 and 30 °C (Figure 1a). At higher temperatures (45 and 60 °C), as shown in Figure 7c,d, the chain-extension profiles clearly show the difference between pure PSM-d_{31} and the cholesterol mixtures, yet surprisingly, almost identical projected chain lengths are calculated for $X_C = 0.2$ and $X_C = 0.33$. It is also interesting that the largest difference between the two cholesterol mixtures is observed for the interfacial region ($i = 2-5$), despite the near saturation of the ordering effect for the other chain segments. This indicates that cholesterol is located directly in the vicinity of the water interface, as already implied by the recent literature.[33] In this regard, cholesterol can be considered as a spacer molecule that increases the separation between the lipid polar headgroups.[34]

However, for POPC-d_{31}, as shown in Figure 8, striking differences in chain packing upon interaction with cholesterol in binary mixtures become evident upon comparison with the results for PSM-d_{31}. The acyl chains of the glycerophospholipid clearly are not affected as strongly as the sphingolipid by the rigid sterol backbone at low cholesterol concentrations. In addition, a more continuous dependence of chain order on cholesterol concentration becomes observable in the case of POPC. This is obviously due to the less favorable interaction of the unsaturated acyl chain of POPC with cholesterol, as has already been shown for different unsaturated lipids.[29,30,35-37] The exact basis for the diminished ordering effect of cholesterol on POPC at intermediate concentrations could have several origins. Molecular dynamics simulations have shown that the hydroxyl group of cholesterol displays a preferential interaction with the carbonyl oxygen of the ester bond in the oleoyl chain of POPC,[38] where the molecularly rough β side of cholesterol would be associated with the oleoyl chain, while the smooth α side could have a preferential interaction with saturated chains.[39] However, at higher cholesterol concentrations ($X_C = 0.33$), the amount of the sterol seems to be sufficient to induce the same order as in a PSM/cholesterol system, as also observed in other studies.[32] It should be noted that the *N*-palmitoyl chain in PSM structurally corresponds more to the *sn*-1 acyl chain of a comparable glycerophospholipid. Direct comparison of the chain length to that of the *sn*-2 palmitoyl chain in POPC still seems to be justified, as the difference in chain lengths for the *sn*-1 and *sn*-2 chains is minimal (e.g., a 0.15 Å difference for the two chains in DPPC[40]).

In terms of miscibility, comparison of the full chain extents of the two lipids, which indicate their hydrophobic chain lengths in the lipid bilayer, leads to further interesting conclusions. Hydrophobic mismatch (or interfacial-area mismatch) between sphingomyelin and POPC in binary mixtures or in ternary mixtures with cholesterol at $X_C = 0.20$ should lead to detectable phase separation. Conversely, as the values of the chain extent are matched much better in mixtures with higher cholesterol contents, the two lipids should mix almost ideally, at least at low temperatures. This of course assumes that neither of the lipids has a strong influence on the acyl chain order of the other, and (in the case of ternary mixtures) that cholesterol is evenly distributed between POPC and sphingomyelin, as suggested previously.[41,42] Additionally, POPC has a stronger tendency than PSM to become disordered at higher temperatures.

The first-order mean-torque model[13] provides two important structural parameters for lipid bilayers: $\langle A \rangle$, the average area per acyl chain, and D_C, the hydrophobic thickness of one bilayer

leaflet. Both quantities are useful for following the expansion of the acyl chains perpendicular or parallel to the membrane normal (director). Figure 9 shows the semilogarithmic temperature dependence of $\langle A \rangle$ and D_C for the two lipids. The phase transition in PSM-d_{31} is suppressed by stepwise addition of cholesterol, as indicated by a sudden increase in area or decrease in hydrophobic thickness with increasing temperature (Figure 9a,c). In contrast, POPC-d_{31} shows a small curvature in this temperature region (Figure 9b,d) at very high cholesterol concentrations. This implies that at high temperatures, the binary POPC-d_{31}/cholesterol mixture with $X_C = 0.33$ undergoes a change from a pure l_o phase to one with greater longitudinal order. Conversely, for PSM-d_{31}, a cholesterol concentration of $X_C = 0.33$ seems to be sufficient to stabilize the l_o phase over the whole temperature range studied. Another observation of interest is that the slopes of the semilogarithmic plots are steeper for POPC-d_{31} than for PSM-d_{31} in a one-phase region. The more pronounced temperature dependence of POPC-d_{31} should further drive phase separation in ternary mixtures at high temperatures. A summary of the structural parameter values obtained for the pure lipids and their binary mixtures with cholesterol by use of the first-order mean-torque model is provided in the Supporting Information.

Ideal or Nonideal Mixing of Sphingomyelin, Phosphatidylcholine, and Cholesterol

By calculating the hydrophobic thicknesses of the palmitoyl chain in the two lipids, it is straightforward to obtain a descriptive and easily interpretable picture of phase separation in the ternary mixtures. Figure 10 gives a first view of the temperature dependence of D_C in different mixtures of PSM-d_{31} and cholesterol and immediately shows the usefulness of the model. In the s_o phase close to the phase transition and in the solid-disordered (s_d) phase, the lipids undergo rotational diffusion about the bilayer normal, so the mean-torque model can be applied. Although a biaxial contribution is not evident, a detailed analysis may require a modification of the formalism. The phase transition of pure PSM-d_{31} at 38 °C can be readily observed in Figure 10a by the sudden increase in D_C from 15.9 Å, which is characteristic of the l_d phase of sphingomyelin, to 19.8 Å, which corresponds to the hydrophobic thickness of a membrane in the s_o phase. At a cholesterol mole fraction of $X_C = 0.15$, the phase-transition temperature is decreased to 34 °C (Figure 2a), which is the typical effect of adding a solute to a pure material. In contrast, at a cholesterol mole fraction of $X_C = 0.25$, the onset of the broadened phase-transition temperature is now at 45 °C, which is evident in Figure 2c. This observation can be explained easily by assuming that the transition is not between an l_d phase and an s_o phase but rather marks the end point of phase separation between l_d and l_o phases, as already implied by the ^{2}H NMR spectra shown earlier. The D_C values provide further evidence that sphingomyelin forms an l_o phase and not an s_o phase at low temperatures and high cholesterol concentrations. While the s_o phase in pure PSM-d_{31} is typified by a chain length of 19.9 Å in Figure 10, the l_o phase of sphingomyelin in a binary mixture with $X_C = 0.33$ exhibits a slightly but distinctly smaller hydrophobic width of 19.5 Å at 20 °C. By addition of such large amounts of cholesterol, the phase separation seems to be suppressed over a large temperature range. Only at temperatures above 38 °C is there a small kink in the temperature dependence of D_C, suggesting that small amounts partition into an l_d phase coexisting with the much larger fraction of l_o domains.

The effect of cholesterol on the average hydrophobic length of the palmitoyl chain in a POPC membrane is again distinct from that in sphingomyelin, as evinced by Figure 10b. The value for D_C at 15 °C increases from 14.8 Å in pure POPC-d_{31} to 19.2 Å at a mole fraction of $X_C = 0.33$, indicating an l_o phase for which D_C is, however, 0.3 Å smaller than in a comparable PSM-d_{31} membrane. At $X_C = 0.33$, the slope of D_C versus temperature changes between 35 and 40 °C, thereby suggesting the appearance of POPC-d_{31} in a more disordered state. Again, the main difference is that the ordering effect of cholesterol is less distinct for POPC-d_{31} than for PSM-d_{31} at the intermediate mole fraction of $X_C = 0.2$. At temperatures of 35−60 °C, the hydrophobic

thickness is 1.7 Å smaller on average for POPC-d_{31} than for PSM-d_{31}, which remains in the presence of cholesterol. Different ordering effects of cholesterol on PSM and POPC are suggested as the driving force behind the acyl length mismatch and therefore the phase separation.

In ternary mixtures, the mean-torque model can provide us with additional arguments for answering the question of whether the lipids are in coexisting phases having different segmental orientational order. As observed by atomic force microscopy in comparable systems,[43] the microdomains consisting of sphingomyelin and cholesterol are distinguished by an increased bilayer thickness compared with that in the surrounding fluid phase. This should be directly observable by a difference in D_C calculated for the two lipids, one participating in the l_d phase and the other in the l_o phase. Another interesting question is whether the phase behavior of the binary systems allows predictions for the ternary systems or a greater affinity between some components leads to different properties. In order to answer these questions, we first examine the plots of the temperature dependence of D_C for ternary mixtures of 1:1 PSM-d_{31}/POPC with cholesterol (Figure 10c). In the cholesterol-free 1:1 binary mixture of PSM-d_{31} and POPC, a phase transition at ~25 °C results in a sudden increase of the hydrophobic thickness from 16.2 to 19.1 Å. This phase transition becomes less pronounced with increasing cholesterol mole fraction and completely vanishes for $X_C \geq 0.33$. Only a slight increase in D_C (0.3 Å) was obtained upon increasing the cholesterol mole fraction to $X_C = 0.5$, indicating that the chain-ordering effect is nearly at a maximum when the cholesterol concentration reaches $X_C = 0.33$.

However, the corresponding plot for POPC-d_{31} in mixtures with sphingomyelin and cholesterol (Figure 10d) shows a completely different picture. For the 1:1 binary mixture of EYSM and POPC-d_{31} in the absence of cholesterol, the acyl chain of POPC displays a clearly smaller hydrophobic thickness than does that of sphingomyelin. Whereas sphingomyelin undergoes a clear phase transition in the binary mixture at 30 °C, the POPC-d_{31} in the same mixture does not deviate from its monotonic dependence of order on temperature. This result, together with the chain-extension profiles displayed in Figure 8a–d, indicates only a small partitioning of sphingomyelin into the l_d phase mainly formed by POPC. Obviously, no ideal mixing between the two components takes place over a broad temperature range. However, the difference of almost 1 Å in the hydrophobic chain lengths at 30 °C does not seem to be enough to completely exclude sphingomyelin from the much more disordered POPC phase, as can be seen in Figure 1c. The addition of cholesterol seems to strengthen this phase separation at first. The difference in hydrophobic thicknesses then increases from 1.6 Å at 60 °C to 4.4 Å at 15 °C. It should be noted that the jump in the temperature dependence for $X_C = 0.2$ in the plot for PSM-d_{31} (Figure 10c) is reflected in the curve for POPC-d_{31} in the identical mixture (Figure 10d). For the sphingolipid, the chain length suddenly increases with decreasing temperature starting at ~25 °C, indicating the emergence of an l_o phase with a larger cholesterol mole fraction. However, for POPC-d_{31}, we see the contrary behavior at 25 °C. Instead of increasing, the thickness decreases at 25 °C, manifesting a decreased order of the palmitoyl chain comparable to that in a pure POPC phase. Although cholesterol is distributed evenly between the two lipids at higher temperatures, it now participates to a greater extent in the l_o phase of sphingomyelin, thereby increasing its order and leaving POPC in a phase of low cholesterol content. This can be explained by a slightly stronger affinity of cholesterol for the sphingolipid. Thus, the thermal energy of the lipids is not sufficient at lower temperatures to overcome the binding enthalpy between cholesterol and sphingomyelin.

The incorporation of cholesterol up to a mole fraction of $X_C = 0.33$ leads to the following interesting effect in ternary mixtures. Although the addition of cholesterol initially drives the phase separation by inducing greater lateral order in sphingomyelin than in POPC, in mixtures with high amounts of cholesterol, saturation of the ordering effect for PSM seems to facilitate mixing of the components. This is indicated by the similarity of the ^{2}H NMR spectra obtained

for the two lipids (Figure 5c,d) as well as by their nearly identical D_C values at lower temperatures (19.3 vs 19.6 Å, respectively, at 15 °C). At a higher temperature of 60 °C, the differences in chain length increase to 2 Å, which is also reflected in significant broadening of the respective signals seen in Figure 5c,d. This again shows the stronger temperature dependence of the POPC acyl chain order, as already evident in the binary mixtures. As a rule, the ternary mixture behaves as implied by the results for the binary mixtures with cholesterol. Moreover, the lipids in the ternary mixture have quite similar structural parameters, as expected if cholesterol is almost evenly distributed between them. Phase separation occurs only if the thermal energy of the molecules is lower than the enthalpy of the cholesterol–sphingolipid interaction and the cholesterol concentration is low enough to enable competition between the two lipids for the sterol. The stronger affinity of cholesterol for sphingomyelin is then sufficient to drive the formation of membrane domains. In our work, this phenomenon was observed only at intermediate cholesterol concentrations, as in the ternary mixture of 1:1 PSM/POPC with $X_C = 0.2$ below 25 °C.

Implications for Rafts in Cellular Membranes

Although glycerophospholipids are sufficient to form lipid bilayers,[44] most eukaryotic cells contain sphingolipids and sterols as additional classes of lipids, each available only through elaborate biosyn-thesis. This considerable anabolic expense, as well as the abundance of these lipid classes in the plasma membrane (typically 30−40 mol % cholesterol and 10−20 mol % sphingomyelin[45]), naturally raises the question of their evolution and function in the organization of the bilayer. The implication that the well-known ordering effect of cholesterol for sphingomyelin and other saturated glycerophospholipids leads to lateral phase segregation and microdomains needs further clarification, as the situation in vivo is far too complex to be determined directly. However, the structural properties and phase-transition temperatures of sphingomyelins near body temperature (37 °C) suggest they may play an important role in the formation of specialized domains in membranes such as lipid rafts.[46] The data assembled in this study give some interesting insights into the effect of cholesterol on the lateral organization of such mixtures. The approach of using a model membrane, comprising a lipid that forms a fluid bilayer together with a lipid known to form a more ordered bilayer as well as cholesterol in varying amounts, is probably most accessible as a mimic of biomembranes with a vast number of components.[47] Interestingly, cholesterol has two different functions in our model membrane system: on the one hand, it further increases the hydrophobic mismatch of the lipids at low concentrations and thereby enhances phase separation, and on the other hand, it functions as a mixing agent at high concentrations. This variation in function is interesting, insofar as other sterols which appear in lower organisms, e.g., lanosterol or ergosterol, show acyl chain ordering in POPC-d_{31} up to just 25 mol % sterol.[32] Consequently the saturating behavior seems to be a distinct feature of each lipid in its interaction with a specific sterol. This has already been shown for 1,2-dimyristoyl-*sn*-glycero-3-phosphocholine (DMPC) membranes, in which, contrary to the case for DPPC membranes, cholesterol has smaller ordering effects than ergosterol[48] but greater effects than lanosterol.[49] Additionally, cholesterol has been found to have a much higher mobility between the two leaflets than ergosterol or lanosterol,[50] further indicating a possible role of cholesterol as a mediator of interactions between the different monolayers.

If we now consider the phase separation as being mostly driven by hydrophobic mismatch of the acyl chains of the various lipids, it is normally assumed that the thickness difference is induced by unequal sterol partitioning into the two phases. However, our study shows that this assumption is not needed for lateral segregation to be generated, because the difference in ordering upon addition of cholesterol already seen in binary mixtures is sufficient to drive phase separation. Additional measurements by us (data not shown) and other studies[42] of perdeuterated cholesterol in PSM/POPC/cholesterol mixtures display an intermediate ordering

between those of PSM/cholesterol and POPC/cholesterol, in contrast to the results for the chain-perdeuterated lipids. In line with recent pulse-field-gradient NMR studies of similar systems,[41] this implies that cholesterol is involved in exchange between the different membrane regions that is fast on the NMR time scale (milliseconds to microseconds). Nonetheless, it should be noted that preferential affinity of the sterol for the sphingolipid probably appears at small cholesterol mole fractions and low temperatures, as shown here for PSM-d_{31}/POPC with X_C = 0.20 below 25 °C.

An alternative[41,42] is to consider a different mechanism for phase separation, namely, the influence of the configurational entropy on the partitioning of lipids with disordered acyl chains in the l_d phase. This mechanism assumes that the overall greater order parameters of sphingomyelin should lead to a smaller entropy penalty than for POPC upon interaction with cholesterol. Miscibility of SM/cholesterol mixtures strongly depends on the degree of unsaturation in similar systems employing phosphatidylethanolamine.[37] This effect could not be seen in our systems, however, as the order in the binary POPC-d_{31}/cholesterol systems is far more sensitive to temperature changes than in comparable mixtures of PSM-d_{31}/cholesterol. In ternary mixtures, this should lead to increased phase separation at high temperatures, which could be seen only weakly in our work and in a recent study on very similiar mixtures.[51] The largest domains with distinct detectable subspectra for each phase were observed in mixtures with X_C = 0.20 at low temperatures, indicating a strong influence of enthalpy rather than entropy.

Finally, we note that the phase separation seems to occur mainly in regions with smaller cholesterol mole fractions, with distinct subspectra observable on the ^{2}H NMR time scale. Hence, it is probable that domain size strongly depends in the same way on sterol concentrations. In other words, domains are largest and most stable at intermediate cholesterol content. If our results were to be compared to those for biological membranes with high cholesterol content (up to 50 mol %), it would seem unlikely that patches of l_o domains would be floating in a completely segregated l_d phase in vivo. More probably, the plasma membrane would exist mainly in a highly ordered l_o phase that is interrupted by smaller, more disordered areas of high fluidity. Of course, this does not take into account the possibility of domain formation due to cytoskeleton-linked membrane proteins or the asymmetric distribution of the diverse lipid species throughout the two leaflets of the bilayer. It has been shown in model membranes[52] that formation of such domains entails Gibbs free energies that are much lower than those for protein–lipid interactions, which therefore may indicate a role for proteins in domain formation. Further detailed information regarding protein–lipid interactions can contribute to an understanding of the lateral organization of cellular plasma membranes and how rafts may be implicated in their functional mechanisms.

Supplementary Material

Refer to Web version on PubMed Central for supplementary material.

Acknowledgment

This work was funded by the Deutsche Forschungsgemeinschaft (Sfb 596), the National Institutes of Health (EY012049, EY018891, and HL083187), and the Arizona Biomedical Research Commission. T.B. thanks Prof. Dr. Daniel Huster and Dr. Alexander Vogel for generously providing the de-Pakeing program.

References

1. a Simons K, Ikonen E. Nature 1997;387:569–572. [PubMed: 9177342] b Brown DA, London E. Biochem. Biophys. Res. Commun 1997;240:1–7. [PubMed: 9367871] c Edidin M. Annu. Rev. Biophys. Biomol. Struct 2003;32:257–283. [PubMed: 12543707]

2. a Simons K, Vaz WL. Annu. Rev. Biophys. Biomol. Struct 2004;33:269–295. [PubMed: 15139814] b Riethmüller J, Riehle A, Grassmé H, Gulbins E. Biochim. Biophys. Acta 2006;1758:2139–2147. [PubMed: 17094939] c Jacobson K, Mouritsen OG, Anderson RG. Nat. Cell Biol 2007;9:7–14. [PubMed: 17199125] d Allen JA, Halverson-Tamboli RA, Rasenick MM. Nat. Rev. Neurosci 2007;8:128–140. [PubMed: 17195035] e Wilflingseder D, Stoiber H. Front. Biosci 2007;12:2124–2135. [PubMed: 17127449]
3. a Brown DA, Rose JK. Cell 1992;68:533–544. [PubMed: 1531449] b Cinek T, Horejsi V. J. Immunol 1992;149:2262–2270. [PubMed: 1382093]
4. a Schroeder RJ, Ahmed SN, Zhu Y, London E, Brown DA. J. Biol. Chem 1998;273:1150–1157. [PubMed: 9422781] b Ilangumaran S, Hoessli DC. Biochem. J 1998;335:433–440. [PubMed: 9761744] c Green JM, Zhelesnyak A, Chung J, Lindberg FP, Sarfati M, Frazier WA, Brown EJ. J. Cell Biol 1999;146:673–682. [PubMed: 10444074] d Roy S, Luetterforst R, Harding A, Apolloni A, Etheridge M, Stang E, Rolls B, Hancock JF, Parton RG. Nat. Cell Biol 1999;1:98–105. [PubMed: 10559881] e Anderson HA, Hiltbold EM, Roche PA. Nat. Immunol 2000;1:156–162. [PubMed: 11248809]
5. Ipsen JH, Karlström G, Mouritsen OG, Wennerström H, Zuckermann MJ. Biochim. Biophys. Acta 1987;905:162–172. [PubMed: 3676307]
6. London E. Biochim. Biophys. Acta 2005;1746:203–220. [PubMed: 16225940]
7. a Ipsen JH, Mouritsen OG, Zuckermann MJ. Biophys. J 1989;56:661–667. [PubMed: 2819232] b Sankaram MB, Thompson TE. Biochemistry 1990;29:10670–10675. [PubMed: 2176878] c Mouritsen OG, Zuckermann MJ. Lipids 2004;39:1101–1113. [PubMed: 15726825] d Veatch SL, Soubias O, Keller SL, Gawrisch K. Proc. Natl. Acad. Sci. U.S.A 2007;104:17650–17655. [PubMed: 17962417]
8. de Almeida RF, Fedorov A, Prieto M. Biophys. J 2003;85:2406–2416. [PubMed: 14507704]
9. Veatch SL, Keller SL. Biophys. J 2003;85:3074–3083. [PubMed: 14581208]
10. Veatch SL, Leung SS, Hancock RE, Thewalt JL. J. Phys. Chem. B 2007;111:502–504. [PubMed: 17228905]
11. Gawrisch K, Eldho NV, Polozov IV. Chem. Phys. Lipids 2002;116:135–151. [PubMed: 12093539]
12. Brown, MF.; Lope-Piedrafita, S.; Martinez, GV.; Petrache, HI. Modern Magnetic Resonance. Webb, GA., editor. Springer; Berlin: 2006. p. 245-256.
13. Petrache HI, Dodd SW, Brown MF. Biophys. J 2000;79:3172–3192. [PubMed: 11106622]
14. a Barenholz Y, Thompson TE. Biochim. Biophys. Acta 1980;604:129–158. [PubMed: 7000188] b Cutler RG, Mattson MP. Mech. Ageing Dev 2001;122:895–908. [PubMed: 11348657]
15. Veatch SL, Keller SL. Phys. Rev. Lett 2005;94:148101−1–148101−4. [PubMed: 15904115]
16. Mehnert T, Jacob K, Bittman R, Beyer K. Biophys. J 2006;90:939–946. [PubMed: 16284259]
17. Bittman R, Verbicky CA. J. Lipid Res 2000;41:2089–2093. [PubMed: 11108743]
18. Kurze V, Steinbauer B, Huber T, Beyer K. Biophys. J 2000;78:2441–2451. [PubMed: 10777740]
19. Steinbauer B, Mehnert T, Beyer K. Biophys. J 2003;85:1013–1024. [PubMed: 12885648]
20. McCabe M, Wassall S. Solid State Nucl. Magn. Reson 1997;10:53–61. [PubMed: 9472792]
21. Davis JH, Jeffrey KR, Bloom M, Valic MI, Higgs TP. Chem. Phys. Lett 1976;42:390–394.
22. Engel AK, Cowburn D. FEBS Lett 1981;126:169–171. [PubMed: 6894577]
23. Guo W, Kurze V, Huber T, Afdhal NH, Beyer K, Hamilton JA. Biophys. J 2002;83:1465–1478. [PubMed: 12202372]
24. a Nagle JF, Wilkinson DA. Biophys. J 1978;23:159–175. [PubMed: 687759] b Petrache HI, Feller SE, Nagle JF. Biophys. J 1997;72:2237–2242. [PubMed: 9129826] c Armen RS, Uitto OD, Feller SE. Biophys. J 1998;75:734–744. [PubMed: 9675175]
25. Jansson M, Thurmond RL, Barry JA, Brown MF. J. Phys. Chem 1992;96:9532–9544.
26. Calhoun WI, Shipley GG. Biochim. Biophys. Acta 1979;555:436–441. [PubMed: 573625]
27. Huber T, Rajamoorthi K, Kurze VF, Beyer K, Brown MF. J. Am. Chem. Soc 2002;124:298–309. [PubMed: 11782182]
28. a Oldfield E, Meadows M, Rice D, Jacobs R. Biochemistry 1978;17:2727–2740. [PubMed: 687560] b Trouard TP, Alam TM, Zajicek J, Brown MF. Chem. Phys. Lett 1992;189:67–75. c Martinez GV, Dykstra EM, Lope-Piedrafita S, Job C, Brown MF. Phys. Rev. E 2002;66:050902−1–050902−4.

29. Brzustowicz MR, Stillwell W, Wassall SR. FEBS Lett 1999;451:197–202. [PubMed: 10371164]
30. Brzustowicz MR, Cherezov V, Caffrey M, Stillwell W, Wassall SR. Biophys. J 2002;82:285–298. [PubMed: 11751316]
31. Henriksen J, Rowat AC, Brief E, Hsueh YW, Thewalt JL, Zuckermann MJ, Ipsen JH. Biophys. J 2006;90:1639–1649. [PubMed: 16326903]
32. Hsueh Y-W, Chen M-T, Patty PJ, Code C, Cheng J, Frisken BJ, Zuckermann M, Thewalt J. Biophys. J 2007;92:1606–1615. [PubMed: 17142279]
33. Cournia Z, Ullmann GM, Smith JC. J. Phys. Chem. B 2007;111:1786–1801. [PubMed: 17261058]
34. Brown MF, Seelig J. Biochemistry 1978;17:381–384. [PubMed: 619997]
35. Wassall SR, Brzustowicz MR, Shaikh SR, Cherezov V, Caffrey M, Stillwell W. Chem. Phys. Lipids 2004;132:79–88. [PubMed: 15530450]
36. a Huster D, Arnold K, Gawrisch K. Biochemistry 1998;37:17299–17308. [PubMed: 9860844] b Shaikh SR, Brzustowicz MR, Gustafson N, Stillwell W, Wassall SR. Biochemistry 2002;41:10593–10602. [PubMed: 12186543] c Brzustowicz MR, Cherezov V, Zerouga M, Caffrey M, Stillwell W, Wassall SR. Biochemistry 2002;41:12509–12519. [PubMed: 12369842] d Shaikh SR, Cherezov V, Caffrey M, Stillwell W, Wassall SR. Biochemistry 2003;42:12028–12037. [PubMed: 14556634] e Shaikh SR, Cherezov V, Caffrey M, Soni SP, LoCascio D, Stillwell W, Wassall SR. J. Am. Chem. Soc 2006;128:5375–5383. [PubMed: 16620109] f Soni SP, LoCascio DS, Liu Y, Williams JA, Bittman R, Stillwell W, Wassall SR. Biophys. J 2008;95:203–214. [PubMed: 18339742]
37. Shaikh SR, Dumaual AC, Castillo A, LoCascio D, Siddiqui RA, Stillwell W, Wassall SR. Biophys. J 2004;87:1752–1766. [PubMed: 15345554]
38. Aittoniemi J, Niemelä PS, Hyvönen MT, Karttunen M, Vattulainen I. Biophys. J 2007;92:1125–1137. [PubMed: 17114220]
39. a Pitman MC, Suits F, Mackerell AD Jr. Feller SE. Biochemistry 2004;43:15318–15328. [PubMed: 15581344] b Pandit SA, Jakobsson E, Scott HL. Biophys. J 2004;87:3312–3322. [PubMed: 15339797] c Huang, C.-h. Lipids 1977;12:348–356. [PubMed: 558491]
40. Pastor RW, Venable RM, Feller SE. Acc. Chem. Res 2002;35:438–446. [PubMed: 12069629]
41. Lindblom G, Orädd G, Filippov A. Chem. Phys. Lipids 2006;141:179–184. [PubMed: 16580657]
42. Aussenac F, Tavares M, Dufourc EJ. Biochemistry 2003;42:1383–1390. [PubMed: 12578350]
43. a Giocondi MC, Boichot S, Plenat T, Le Grimellec CC. Ultramicroscopy 2004;100:135–143. [PubMed: 15231303] b Giocondi MC, Milhiet PE, Dosset P, Le Grimellec C. Biophys. J 2004;86:861–869. [PubMed: 14747321]
44. Bloom M, Evans E, Mouritsen OG. Q. Rev. Biophys 1991;24:293–397. [PubMed: 1749824]
45. a Lange Y, Swaisgood MH, Ramos BV, Steck TL. J. Biol. Chem 1989;264:3786–3793. [PubMed: 2917977] b van Meer G. Annu. Rev. Cell Biol 1989;5:247–275. [PubMed: 2688705]
46. Barenholz Y, Thompson TE. Chem. Phys. Lipids 1999;102:29–34. [PubMed: 11001558]
47. Feigenson GW. Nat. Chem. Biol 2006;2:560–563. [PubMed: 17051225]
48. Urbina JA, Pekerar S, Le H.-b. Patterson J, Montez B, Oldfield E. Biochim. Biophys. Acta 1995;1238:163–176. [PubMed: 7548131]
49. Martinez GV, Dykstra EM, Lope-Piedrafita S, Brown MF. Langmuir 2004;20:1043–1046. [PubMed: 15803674]
50. Endress E, Heller H, Casalta H, Brown MF, Bayerl TM. Biochemistry 2002;41:13078–13086. [PubMed: 12390036]
51. Bunge A, Müller P, Stöckl M, Herrmann A, Huster D. Biophys. J 2008;94:2680–2690. [PubMed: 18178660]
52. a Huang J, Swanson JE, Dibble AR, Hinderliter AK, Feigenson GW. Biophys. J 1993;64:413–425. [PubMed: 8457667] b Jerala R, Almeida PF, Biltonen RL. Biophys. J 1996;71:609–615. [PubMed: 8842200] c Sugar IP, Thompson TE, Biltonen RL. Biophys. J 1999;76:2099–2110. [PubMed: 10096905] d Tokutake N, Jing B, Regen SL. J. Am. Chem. Soc 2003;125:8994–8995. [PubMed: 15369338] e Almeida PF, Pokorny A, Hinderliter A. Biochim. Biophys. Acta 2005;1720:1–13. [PubMed: 16472555]

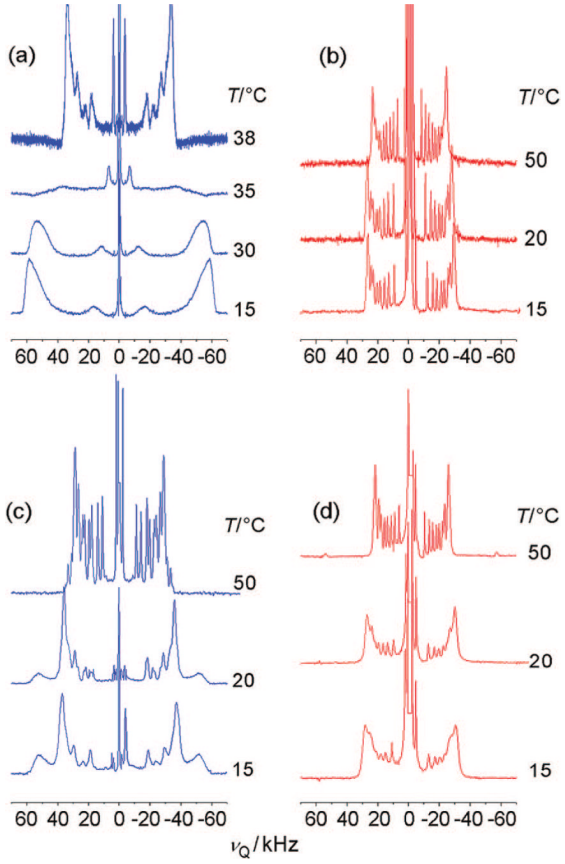

Figure 1.

Solid-state ^{2}H NMR spectra as a function of temperature demonstrate phase transitions of pure lipids and lipids in binary mixtures: (a) PSM-d_{31}; (b) POPC-d_{31}; (c) 1:1 PSM-d_{31}/POPC; and (d) 1:1 EYSM/POPC-d_{31}. Macroscopically oriented samples ($\theta = 0°$) were hydrated with 10:90 (v/v) $^2H_2O/^1H_2O$ to a final water/lipid molar ratio of 25, as detailed in Methods. Note the sharp phase transition in (a) at 38 °C and the emergence of an additional spectral component in (c).

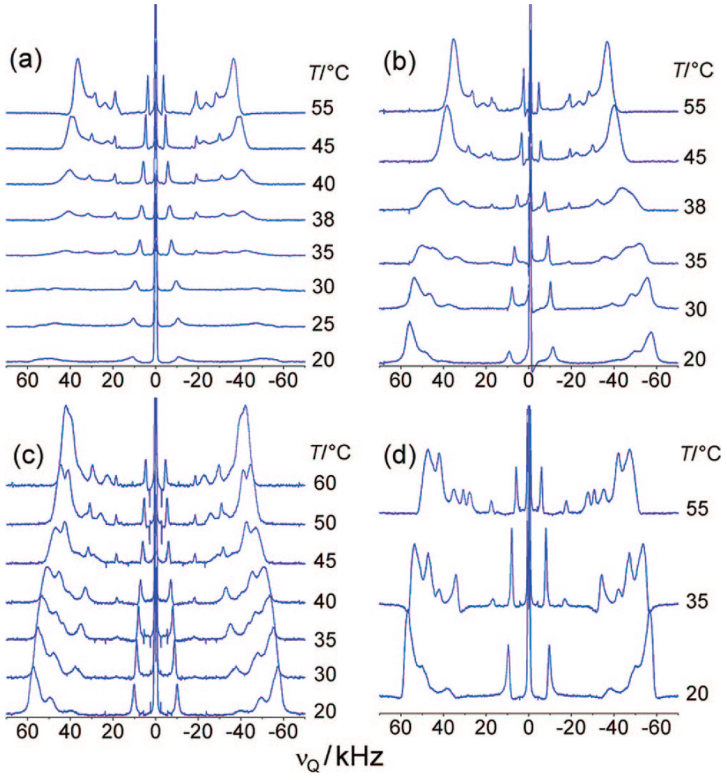

Figure 2.

Cholesterol leads to broadening or disappearance of the s_o phase of PSM, as shown by solid-state ^{2}H NMR spectra of PSM-d_{31}/cholesterol with X_C = (a) 0.15, (b) 0.20, (c) 0.25, and (d) 0.33. Oriented samples (θ = 0°) in (a–d) contained 10:90 (v/v) $^2H_2O/^1H_2O$ and a water/lipid molar ratio of at least 25.

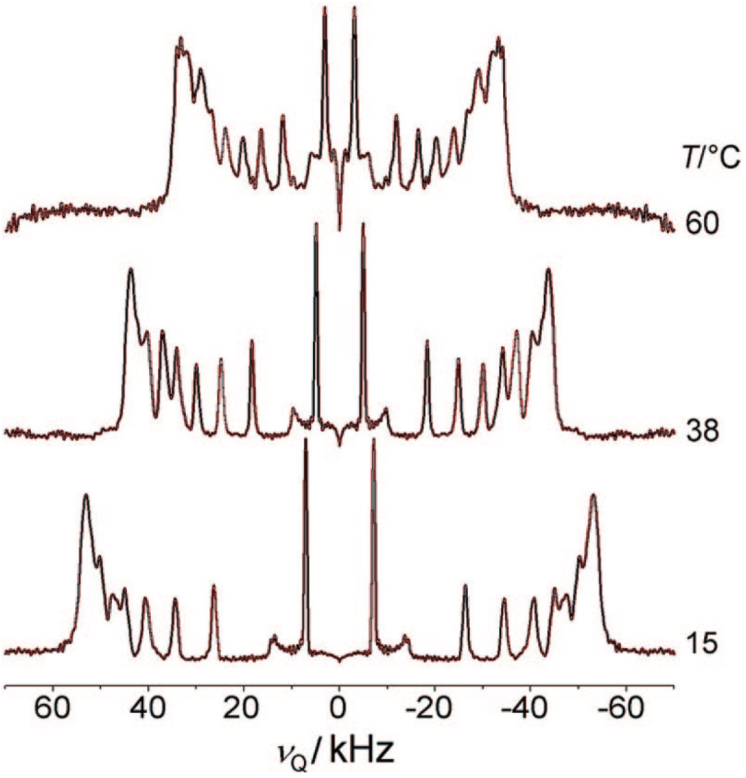

Figure 3.
De-Paked ^{2}H NMR spectra of a POPC-d_{31}/cholesterol mixture with X_C = 0.33 at various temperatures. The powder-type samples contained 50 wt % ^1H_2O. Note the similiarity to the PSM-d_{31} spectrum at low temperatures (Figure 2d).

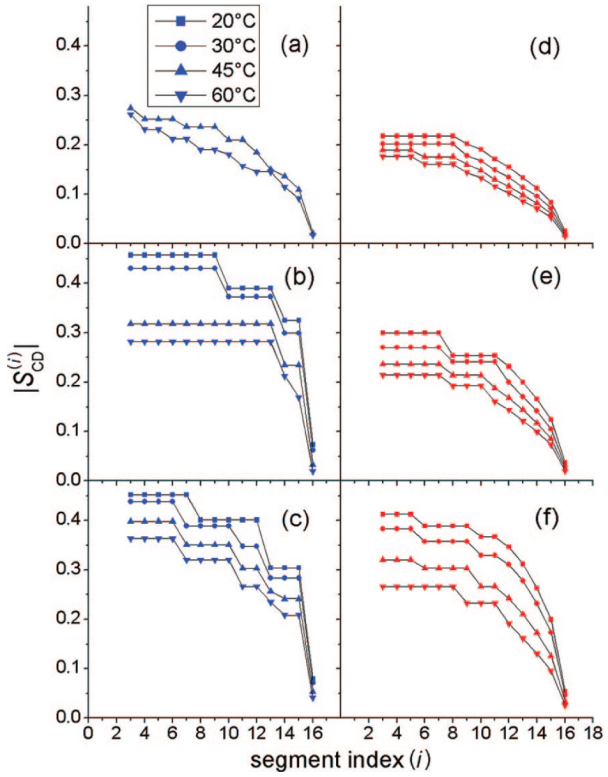

Figure 4.

Order parameters $|S_{CD}^{(i)}|$ vs carbon segment *i* for chain-deuterated PSM and POPC alone and in binary lipid/cholesterol mixtures: (a) PSM-d_{31} alone; (b) PSM-d_{31}/cholesterol, $X_C = 0.20$; (c) PSM-d_{31}/cholesterol, $X_C = 0.33$; (d) POPC-d_{31} alone; (e) POPC-d_{31}/cholesterol, $X_C = 0.20$; and (f) POPC-d_{31}/cholesterol, $X_C = 0.33$. Note that the largest differences in orientational order of POPC and PSM occur at intermediate cholesterol mole fractions.

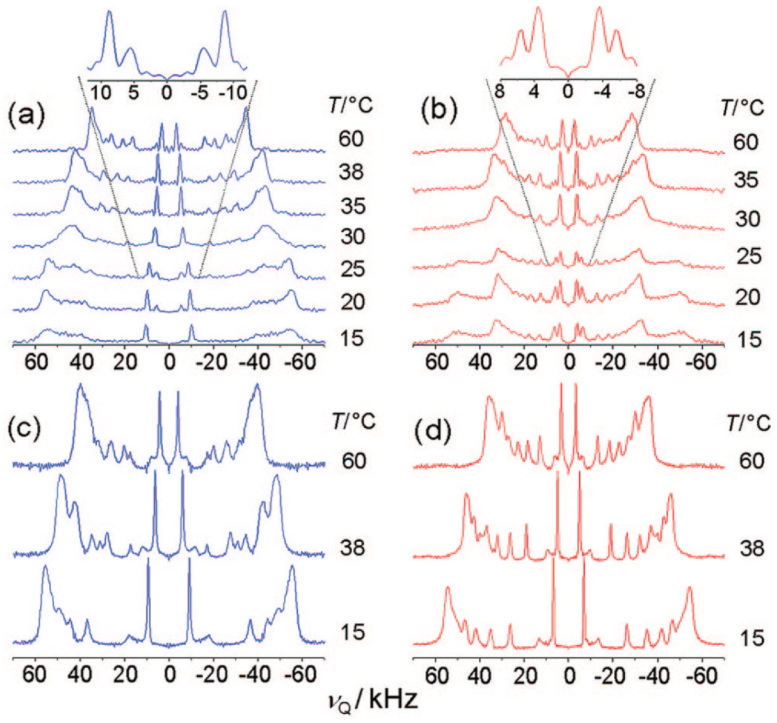

Figure 5.

De-Paked solid-state ^{2}H NMR spectra of ternary raftlike mixtures as a function of temperature show phase separation: (a) 1:1 PSM-d_{31}/POPC, $X_C = 0.2$; (b) 1:1 EYSM/POPC-d_{31}, $X_C = 0.2$; (c) 1:1 PSM-d_{31}/POPC, $X_C = 0.33$; and (d) 1:1 EYSM/POPC-d_{31}, $X_C = 0.33$. The insets in (a) and (b) show expansions of the methyl group signal at 25 °C. Powder-type samples contained 50 wt % ^1H_2O. Note that for $X_C = 0.2$, discrete components due to POPC-d_{31} and PSM-d_{31} phase separation are observed at lower temperatures, whereas for $X_C = 0.33$, the lipids mix almost ideally.

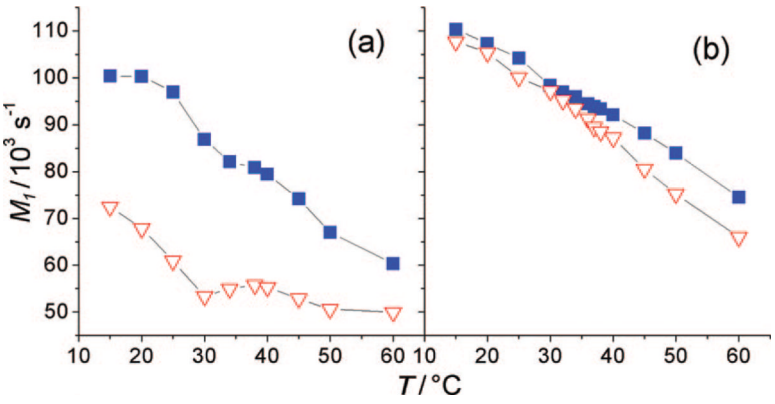

Figure 6.

First spectral moments of powder-type samples as a function of temperature reveal phase separation. Data are shown for mixtures of 1:1 PSM-d_{31}/POPC (■) and 1:1 EYSM/POPC-d_{31} (▽) with cholesterol for (a) $X_C = 0.2$ and (b) $X_C = 0.33$. The overall ordering of the acyl chain in POPC-d_{31} is significally different from that in PSM-d_{31} in ternary mixtures with $X_C = 0.2$ but almost the same for $X_C = 0.33$.

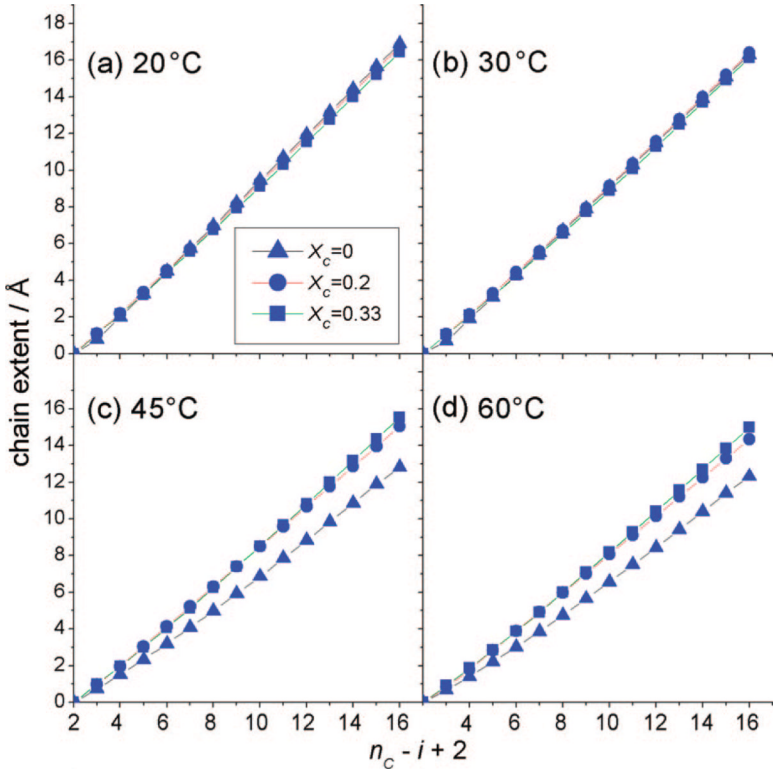

Figure 7.

Segmental projections onto the bilayer normal for PSM-d_{31}/cholesterol binary mixtures at different temperatures reveal the effect of cholesterol on the orientational order of PSM-d_{31} chains. The indexing ($n_C - i + 2$) starts from the terminal methyl group ($i = n_C$) and ends at the C2 carbon ($i = 2$). Data are shown for pure PSM-d_{31} (▲), PSM-d_{31} with $X_C = 0.2$ (●), and PSM-d_{31} with $X_C = 0.33$ (■) at temperatures of (a) 20, (b) 30, (c) 45, and (d) 60 °C. The chain extent of the l_o state corresponds to that of the s_o phase, where the full chain length of the l_o state is reached at $X_C = 0.2$. The full chain extent corresponds to $\langle L_C^* \rangle$ from eq 5.

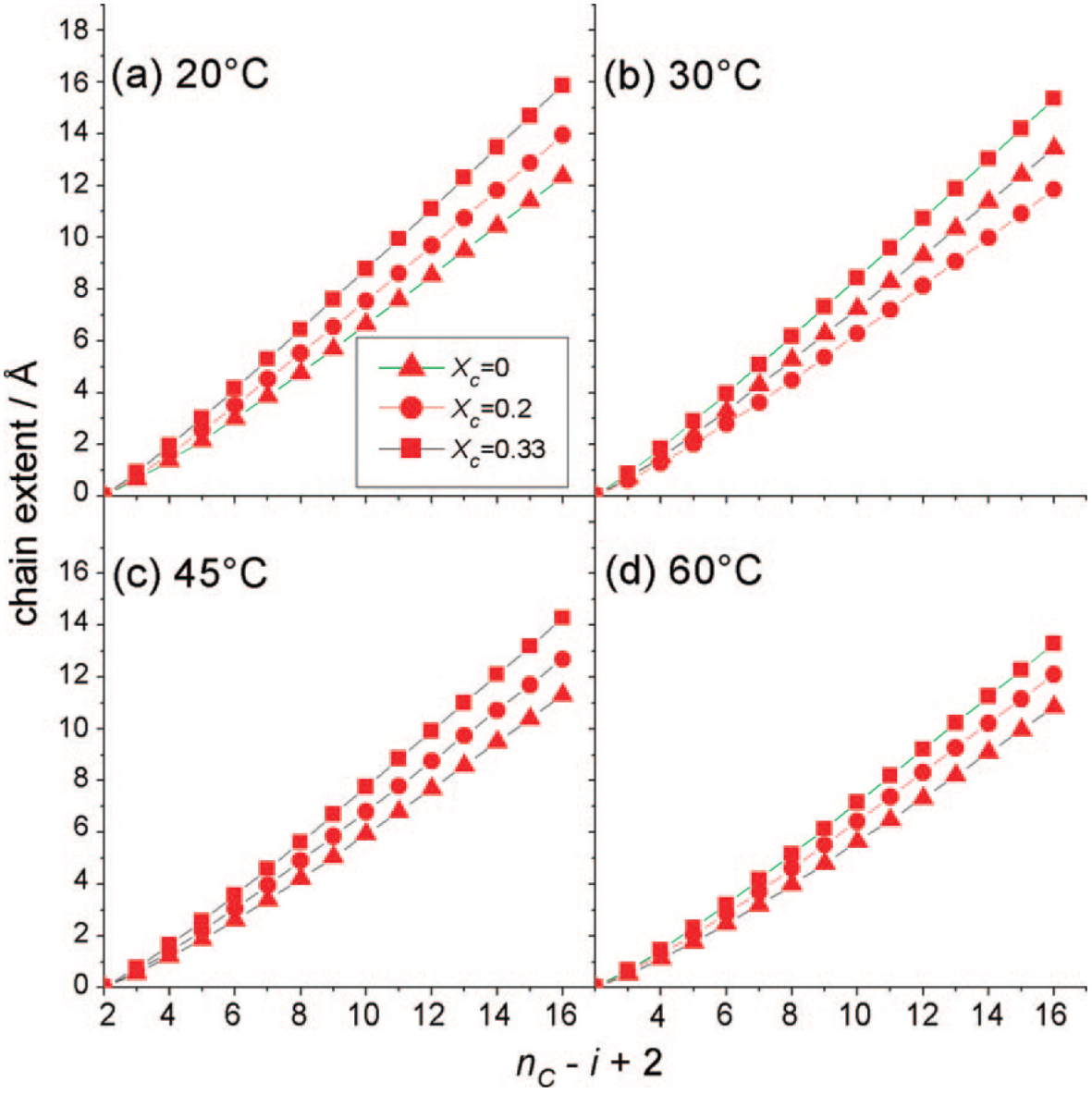

Figure 8.

Chain-extension profiles (cumulative segmental projections) for POPC-d_{31}/cholesterol binary mixtures show the influence of cholesterol on the orientational order of POPC-d_{31} acyl groups. The indexing ($n_C - i + 2$) begins with the terminal methyl group ($i = n_C$) and ends at the C2 carbon ($i = 2$). Results are shown for pure POPC-d_{31} (▲), POPC-d_{31} with $X_C = 0.2$ (●), and POPC-d_{31} with $X_C = 0.33$ (■) at temperatures of (a) 20, (b) 30, (c) 45, and (d) 60 °C. For POPC-d_{31}, the chain length markedly depends on the cholesterol concentration.

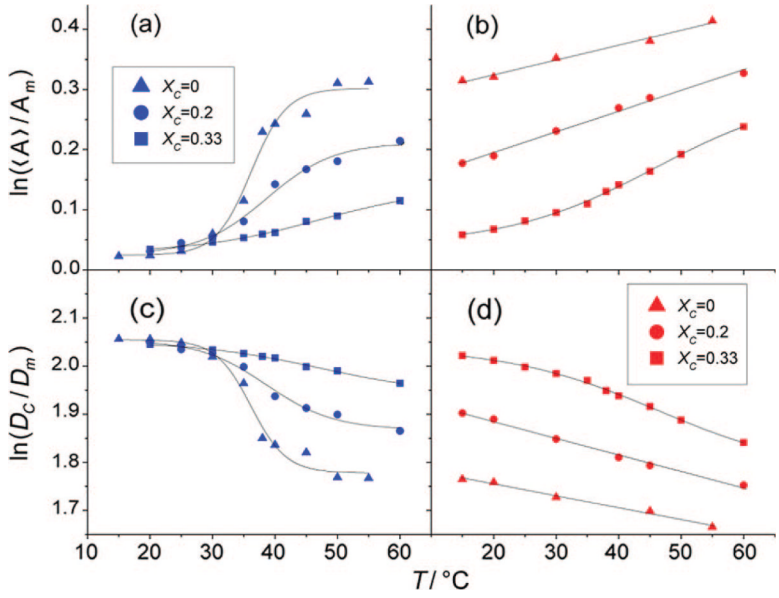

Figure 9.

Semilogarithmic plots of relative variation of (a, b) the average area per lipid $\langle A \rangle$ and (c, d) the hydrophobic thickness D_C (as calculated from the plateau splittings of the respective mixtures) vs temperature. The effect of cholesterol on the phase transitions of (a, c) PSM-d_{31} and (b, d) POPC-d_{31} in binary mixtures is shown: pure lipid (▲), X_C = 0.2 (●), and X_C = 0.33 (■). Increasing the cholesterol concentration diminishes the phase transition of PSM-d_{31} but may promote a phase transition in POPC-d_{31} at X_C = 0.33, as indicated by a small curvature of the plots. Note that the plots are always steeper for POPC-d_{31} than for PSM-d_{31} in a one-phase regime.

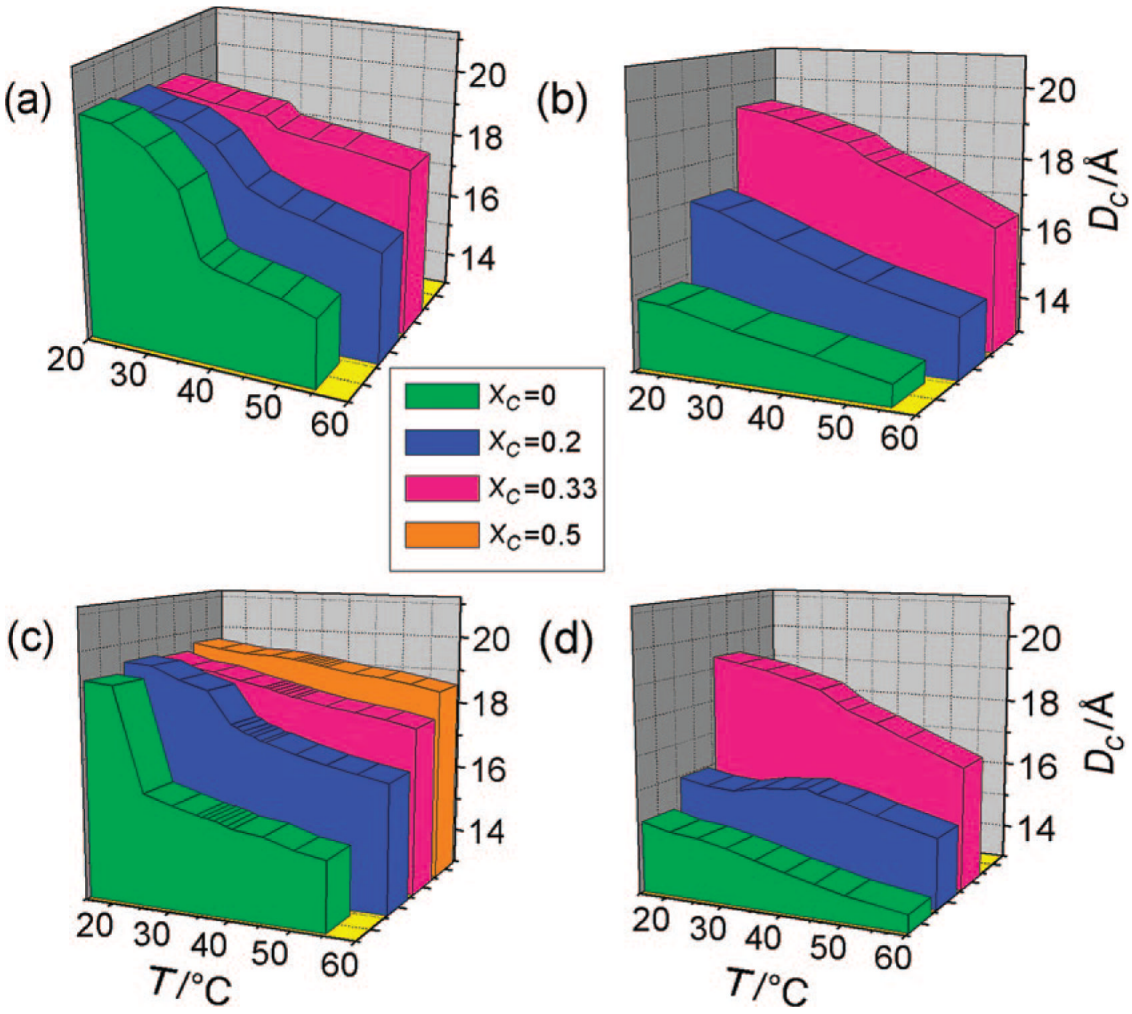

Figure 10.

Chain thickness D_C as a function of temperature and cholesterol concentration: (a) PSM-d_{31}; (b) POPC-d_{31}; (c) 1:1 PSM-d_{31}/POPC; and (d) 1:1 EYSM/POPC-d_{31}. Application of the mean-torque model shows the influence of hydrophobic mismatch at intermediate cholesterol mole fractions, leading to formation of lipid rafts. Phase transitions are seen as a jump in the temperature dependence of D_C. In ternary mixtures with intermediate cholesterol concentrations, the hydrophobic mismatch between POPC-d_{31} and PSM-d_{31} becomes evident. Note that the hydrophobic thickness in the ternary mixtures approximately corresponds to the values in the binary samples. This implies an equal distribution of cholesterol between the two lipids.